

Upper critical fields of superconductor-ferromagnet multilayers

Z. Radović and L. Dobrosavljević-Grujić

Department of Physics, Faculty of Science, Institute of Physics, Belgrade, Yugoslavia

A. I. Buzdin

Physics Department, Moscow State University, Moscow, Union of Soviet Socialist Republics

John R. Clem

Ames Laboratory and Department of Physics, Iowa State University, Ames, Iowa 50011

(Received 29 January 1988)

Nucleation of the superconducting phase in superconductor-ferromagnet multilayers is studied theoretically. When the superconducting layers are thin and decoupled by pair breaking in the ferromagnetic layers, the parallel critical field exhibits a nonlinear temperature dependence and non-monotonic thickness dependence. The perpendicular critical field, corresponding to the nucleation of strongly modulated vortices, is also calculated. The theoretical results are in good agreement with experimental data for V/Fe multilayers.

I. INTRODUCTION

Among artificially layered superconductors,¹ the study of alternately stacked superconducting (S) and magnetic (M) layers is of considerable interest. Such multilayer structures, as for example, V/Fe (Refs. 2 and 3) and Mo/Ni (Ref. 4) are ideal model systems for studying the interplay of superconductivity and magnetism, and may also contribute to the understanding of multiphase high-temperature superconductors. In this paper we calculate the critical temperatures and the upper critical fields of superconductor-ferromagnet (S/M) multilayer structures, both parallel ($H_{c2\parallel}$) and perpendicular ($H_{c2\perp}$) to the layers.

The first attempts to calculate the critical fields of metallic multilayers near the critical temperature T_c have been made by using the anisotropic Ginzburg-Landau (GL) equations, treating the superlattice as an anisotropic superconductor.¹ In such an approach, the temperature dependence of $H_{c2\parallel}$ is expected to be linear. With decreasing temperature, dimensional crossover from three-dimensional (3D) to two-dimensional (2D) behavior is expected when the effective perpendicular coherence length ξ_{\perp} becomes smaller than the thickness d_N of the normal (N) metal, separating the S films. However, a 3D behavior may not occur when the normal-metal layers are ferromagnetic. In S/M superlattices,²⁻⁴ where $\xi_{\perp} \gg d_N$, $H_{c2\parallel}(T)$ shows a square-root temperature dependence near T_c , typical for thin and isolated superconducting films.⁵ To explain this feature, and strong decrease of T_c , we take into account the proximity-induced magnetic pair breaking in S films.

Recently, Takahashi and Tachiki⁶ developed a method for the calculation of $H_{c2}(T)$ of S/N multilayers, based on de Gennes's microscopic approach. However, these authors did not evaluate $H_{c2}(T)$ for the case of S/M multilayers.

We present here, in Sec. II, a general formalism suitable for the study of S/M proximity systems, based on the dirty-limit version of Eilenberger theory.⁷ Similar formalism was applied by Biagi *et al.*⁸ to the study of S/N multilayers and by Buzdin *et al.*⁹ to the problem of superconducting domain walls in ferromagnets. In Sec. III we evaluate T_c and $H_{c2\parallel}(T)$ of a single S film embedded in M metal, assuming that the S film is thin enough that no vortices appear in it. We apply this result to S/M superlattices with strongly decoupled thin S layers. The calculation of T_c in the general case is done in Ref. 10. Following Ref. 8, in Sec. IV we calculate $H_{c2\perp}(T)$ corresponding to the nucleation of vortices, whose cores are strongly modulated in the field direction. We show that in the present case the ratio $H_{c2\perp}/H_{c2\parallel}$ is temperature independent. We compare the theory with experimental data for V/Fe and discuss our results in Sec. V.

II. GENERAL CONSIDERATIONS

Assuming that both S and M metals are dirty, we use the quasiclassical equations⁷ for the Gorkov's Green's functions integrated over energy and averaged over the Fermi surface, $F(\mathbf{r}, \omega)$ and $G(\mathbf{r}, \omega)$. The functions F and G describe the condensate of pairs and the normal excitations, respectively. Near the second-order phase transition at $H_{c2}(T)$, we have $|F| \ll 1$, and $G \approx 1$, such that F is given by the linearized equation

$$-\frac{D}{2}\nabla^2 F = \frac{\Delta}{\hbar} - \omega F. \quad (1)$$

Here, $\Delta = \Delta(\mathbf{r})$ is the pair potential, D is the diffusion coefficient, $\hbar\omega = \pi k_B T(2n + 1)$ with $n = 0, 1, 2, \dots$, and $\nabla = \nabla + 2\pi i \mathbf{A}/\Phi_0$ is the gauge-invariant gradient with vector potential \mathbf{A} and flux quantum Φ_0 .

Equation (1) should be completed by the self-consistency condition relating Δ to F :

$$\Delta \ln \frac{T_{c0}}{T} = 2\pi k_B T \sum_{\omega} \left[\frac{\Delta}{\hbar\omega} - F \right], \quad (2)$$

where T_{c0} represents the bulk critical temperature of either metal, i.e., T_{cS} or T_{cM} .

Using the ansatz

$$F = \Delta / [\hbar\omega + 2\pi k_B T_{c0} \rho(t)], \quad (3)$$

we find that for the S metal Eq. (1) reduces to

$$\Pi^2 F_S = -k_S^2 F_S, \quad (4)$$

with

$$k_S^2 = 2\rho(t) / \xi_S^2 \quad (5)$$

and

$$\xi_S = (\hbar D_S / 2\pi k_B T_{cS})^{1/2}. \quad (6)$$

Note that Eq. (4) is formally identical to the linearized first GL equation, and that the GL coherence length is related to ξ_S by

$$\xi(T) = \frac{\pi}{2} \xi_S (1 - T/T_c)^{-1/2}.$$

Equation (2), which relates the pair-breaking parameter $\rho(t)$ to the reduced temperature $t = T/T_{cS}$, becomes

$$\ln t = \Psi(\frac{1}{2}) - \text{Re}\Psi(\frac{1}{2} + \rho/t), \quad (7)$$

where Re means that the real part has to be taken, and $\Psi(x)$ is the digamma function. Although ρ remains real in S/N proximity systems, it is complex in S/M multilayers because of the exchange field effect. We neglect other possible depairing mechanisms in S , as the Pauli paramagnetism or the spin-orbit scattering. When necessary, these contributions can be easily included in Eq. (7),¹¹ due to the additivity of the pair-breaking parameters.

For M metal where the dominant effect is the polarization of the conduction electrons by the strong exchange field, Eq. (1) holds with $\hbar\omega \rightarrow \hbar\omega + iI_0$,⁹ where I_0 is the exchange energy. Taking $F_M \neq 0$ due to the proximity effect and using Eq. (3) with $\rho/t = -\frac{1}{2}$ corresponding to $T_{cM} = 0$, we obtain

$$\Pi^2 F_M = k_M^2 F_M, \quad (8)$$

with

$$k_M^2 = \frac{2}{\hbar D_M} (\pi k_B T + iI_0). \quad (9)$$

Assuming that $I_0 \gg k_B T_{cS}$, we may take k_M as temperature independent:

$$k_M = (1+i) \frac{2}{\xi_M}, \quad (10)$$

where

$$\xi_M = (4\hbar D_M / I_0)^{1/2} \quad (11)$$

is the characteristic distance of decay of F in M layers. It is worth noting that the decoupling of S films by an M layer is much more effective than by an N layer of the same thickness, since ξ_M is temperature independent and

much smaller than the corresponding length $\xi_N = (\hbar D_N / 2\pi k_B T)^{1/2}$ in a normal metal with $T_{cN} = 0$ and $D_N = D_M$.

To evaluate the critical fields in the general case, Eqs. (4) and (8) should be completed by appropriate boundary conditions at S/M interfaces.¹²

III. PARALLEL CRITICAL FIELD

We confine ourselves to the case of strongly decoupled S layers, thin enough that no vortices appear in them. The problem of $H_{c2\parallel}$ of such multilayers is then reduced to that of a thin S film embedded in a ferromagnet, the nucleation of superconductivity starting in the middle of the film, and F varying in the transverse direction only. Taking the applied magnetic field $\mathbf{H} = H\hat{z}$ parallel to the S film of thickness d_S situated in the y - z plane, we choose the midplane of the film as $x=0$ and use the gauge $\mathbf{A} = (0, Hx, 0)$. When $F(\mathbf{r}) = F(x)$, Eqs. (4) and (8) become

$$\frac{d^2 F_S}{dx^2} - \left[\left(\frac{2\pi H}{\Phi_0} \right)^2 x^2 - k_S^2 \right] F_S = 0, \quad (12a)$$

and

$$\frac{d^2 F_M}{dx^2} - \left[\left(\frac{2\pi H}{\Phi_0} \right)^2 x^2 + k_M^2 \right] F_M = 0. \quad (12b)$$

Taking into account the symmetry of the problem and the boundary condition $|F_M| \rightarrow 0$ for $x \rightarrow \pm\infty$, the solutions of Eqs. (12) can be written as even functions of x :

$$F_S = C_1 e^{-\pi H x^2 / \Phi_0} M \left[\frac{1 - \frac{\Phi_0 k_S^2}{2\pi H}}{4}, \frac{1}{2}, \frac{2\pi H x^2}{\Phi_0} \right], \quad |x| \leq d_S/2 \quad (13a)$$

and

$$F_M = C_2 e^{-\pi H x^2 / \Phi_0} U \left[\frac{1 + \frac{\Phi_0 k_M^2}{2\pi H}}{4}, \frac{1}{2}, \frac{2\pi H x^2}{\Phi_0} \right], \quad |x| > d_S/2 \quad (13b)$$

where $M(a, b, c)$ and $U(a, b, c)$ are Kummer's hypergeometric functions,¹³ and C_1 and C_2 are arbitrary constants.

Solutions (13) are subject to the generalized de Gennes-Werthamer boundary condition¹² at the S/M interfaces:

$$\frac{d}{dx} \ln F_S = \eta \frac{d}{dx} \ln F_M \Big|_{x=\pm d_S/2}. \quad (14)$$

The parameter η characterizes the interfaces. In the dirty limit and for specular scattering, $\eta = \sigma_M / \sigma_S$ is the ratio of the normal-state conductivities.

For a thin S film and strong pair breaking in M , we have $2\pi H x^2 / \Phi_0 < 1$ for $x \leq d_S/2$ and $|k_M x| \gg 1$ for $x \geq d_S/2$, which enables us to use a series expansion for the M function and an asymptotic expression for the U function.¹³ Then, instead of Eqs. (13) we obtain

$$F_S(x) = C_1 \left\{ \cos\phi(x) + \frac{1}{6} \left[\frac{2\pi Hx^2}{\Phi_0} \right]^2 \left[\frac{3 \cos\phi(x)}{2\phi^2(x)} + \frac{\sin\phi(x)}{\phi(x)} \left[1 - \frac{3}{2\phi^2(x)} \right] \right] \right\}, \tag{15a}$$

where

$$\phi(x) = k_S x, \quad 0 < \text{Re}\phi(x) < \pi/2,$$

and

$$F_M(x) = C_2 \exp(-k_M |x|). \tag{15b}$$

The latter approximation of F_M means that the effect of the external field is negligible in comparison with the strong exchange field in M regions. From Eqs. (14) and (15) we obtain for $H_{c2\parallel}$

$$\frac{\phi \sin\phi - \frac{1}{96} \left[\frac{2\pi H_{c2\parallel} d_S^2}{\Phi_0} \right]^2 \left[\cos\phi + \frac{3 \cos\phi}{2\phi^2} + \frac{3 \sin\phi}{2\phi} \left[1 - \frac{1}{\phi^2} \right] \right]}{\cos\phi + \frac{1}{96} \left[\frac{2\pi H_{c2\parallel} d_S^2}{\Phi_0} \right]^2 \left[\frac{3 \cos\phi}{2\phi^2} + \frac{\sin\phi}{\phi} \left[1 - \frac{3}{2\phi^2} \right] \right]} = (1+i) \frac{d_S/\xi_S}{\epsilon}, \tag{16}$$

where $\epsilon = \xi_M/\eta\xi_S$ and $\phi = k_S d_S/2$.

For $H_{c2\parallel} = 0$, Eq. (16) reduces to

$$\phi_0 \tan\phi_0 = (1+i) \frac{d_S/\xi_S}{\epsilon}, \tag{17}$$

where ϕ_0 is the value of ϕ at $T = T_c$. Solving this equation for given d_S/ξ_S and ϵ , and using Eq. (5) rewritten in the form

$$\rho(t_c) = \frac{2\phi_0^2}{(d_S/\xi_S)^2}, \tag{18}$$

we calculate the reduced critical temperature $t_c = T_c/T_{cS}$ from Eq. (7). The results of numerical calculations are shown in Fig. 1. Simple analytical solutions for ϕ_0^2 , and hence for $\rho(t_c)$, can be found only in two limiting cases: relatively thin S films, where $d_S/\xi_S \ll \epsilon$, and relatively thick S films, where $d_S/\xi_S \gg \epsilon$. In the first case, F_S is nearly constant within the film, $|\phi_0| \ll 1$, so that

$$\rho(t_c) = \frac{2}{\epsilon(d_S/\xi_S)} \left[1 + i - \delta_1 \left[\frac{d_S}{\epsilon\xi_S} \right] \right], \tag{19a}$$

with

$$\delta_1(x) = \frac{17}{180}x^2 + i\left(\frac{2}{3}x - \frac{17}{180}x^2\right) + \dots$$

In the second case, F_S is close to zero at the S/M interfaces, $|\pi/2 - \phi_0| \ll 1$, and we obtain

$$\rho(t_c) = \frac{\pi^2/2}{(d_S/\xi_S)^2} \left[1 - \delta_2 \left[\frac{\epsilon\xi_S}{d_S} \right] \right], \tag{19b}$$

with

$$\delta_2(x) = x - \frac{5}{6}x^3 - i\left(x - \frac{3}{2}x^2 + \frac{5}{6}x^3\right) + \dots$$

Note that the superconductivity persists only for d_S larger than a certain critical thickness d_{Sc} ($T_c = 0$ for $d_S \leq d_{Sc}$). The dependence of d_{Sc}/ξ_S on ϵ , shown in Fig. 2, is calculated from Eqs. (17) and (18) by using the asymptotic form $|\rho(0)| = \exp(\Psi \frac{1}{2}) \approx 0.14$ in Eq. (18). In

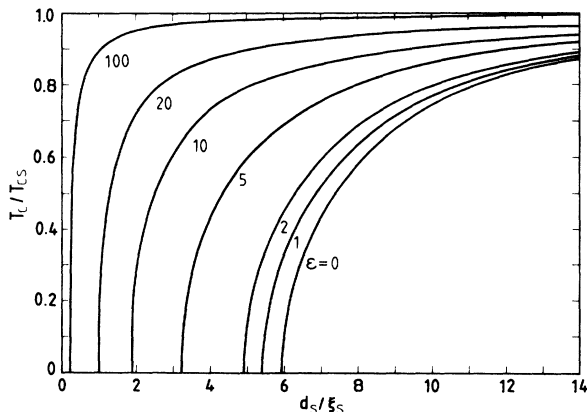


FIG. 1. The reduced critical temperature T_c/T_{cS} as a function of the reduced S film thickness d_S/ξ_S for different values of ϵ .

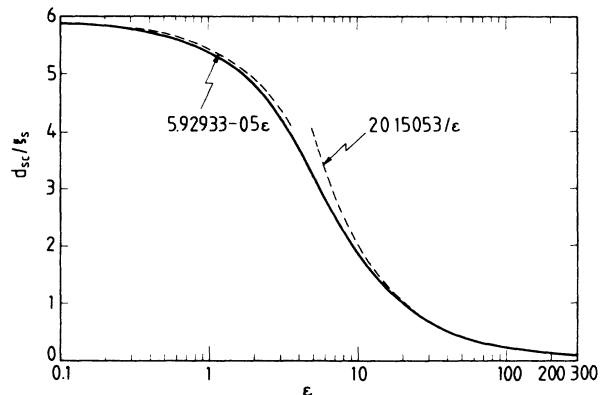


FIG. 2. The reduced critical thickness d_{Sc}/ξ_S vs ϵ . The low and the high ϵ approximations are shown (dashed curves).

particular, for $\epsilon \gg 1$ the critical thickness is given by $d_{Sc}/\xi_S = 20.1505/\epsilon$, and for $\epsilon \ll 1$ by $d_{Sc}/\xi_S = 5.9293 - 0.5\epsilon$.

For $T < T_c$, we calculate ϕ^2 from Eq. (16) to the first order in $(2\pi H_{c2\parallel} d_S^2 / \Phi_0)^2 < 1$ and use Eq. (5) to include in ρ the orbital effect of the magnetic field:

$$\rho(t) = \rho(t_c) + \frac{g(\phi_0)}{24} \left[\frac{2\pi H_{c2\parallel}}{\Phi_0} \right]^2 d_S^2 \xi_S^2. \quad (20)$$

Here $\rho(t_c)$ is given by Eq. (18) and the second term is the same as for a single thin S film in vacuum, except for the factor

$$g(\phi_0) = 1 - \frac{3}{2\phi_0^2} + \frac{3 + 2\phi_0 \tan \phi_0}{\phi_0^2 + \phi_0 \tan \phi_0 + (\phi_0 \tan \phi_0)^2} \\ = \begin{cases} 1; & \phi_0 \rightarrow 0 \\ 1 - 6/\pi^2; & \phi_0 \rightarrow \pi/2. \end{cases} \quad (21)$$

For given d_S/ξ_S and ϵ , $H_{c2\parallel}(t)$ is calculated from Eq. (7) with ρ determined by Eqs. (17)–(21). The results of numerical calculations of $\rho(t) - \rho(t_c)$ for two limiting cases are shown in Fig. 3. The temperature variation of critical fields is illustrated in Fig. 4 for different values of ϵ and d_S/ξ_S . The square-root dependence of $H_{c2\parallel}$ on $(1 - T/T_c)$ in the vicinity of T_c , where the curves

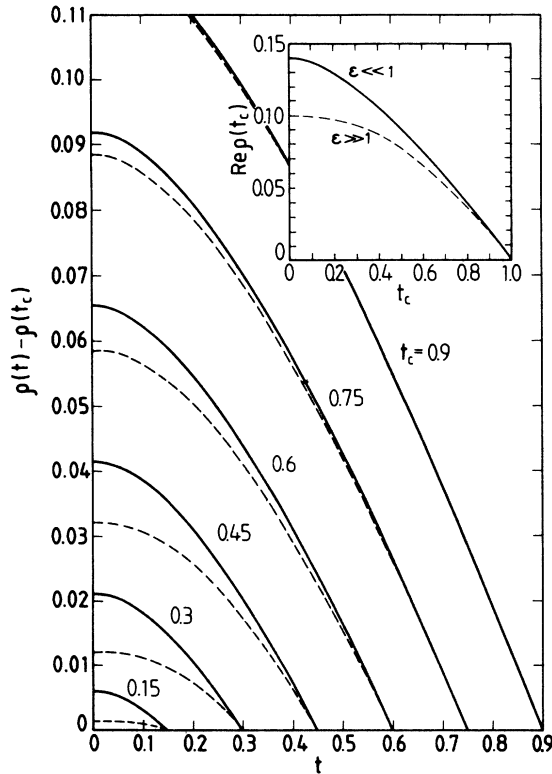


FIG. 3. Graphs of $\rho(t) - \rho(t_c)$ vs $t = T/T_{cS}$ for different values of $t_c = T_c/T_{cS}$ in two limiting cases: $\epsilon \ll 1$ (solid curves) and $\epsilon \gg 1$ (dashed curves). Inset: $\text{Re} \rho(t_c)$ vs t_c . For $\epsilon \ll 1$ $\text{Im} \rho(t_c) = 0$, and for $\epsilon \gg 1$ $\text{Im} \rho(t_c) = \text{Re} \rho(t_c)$.

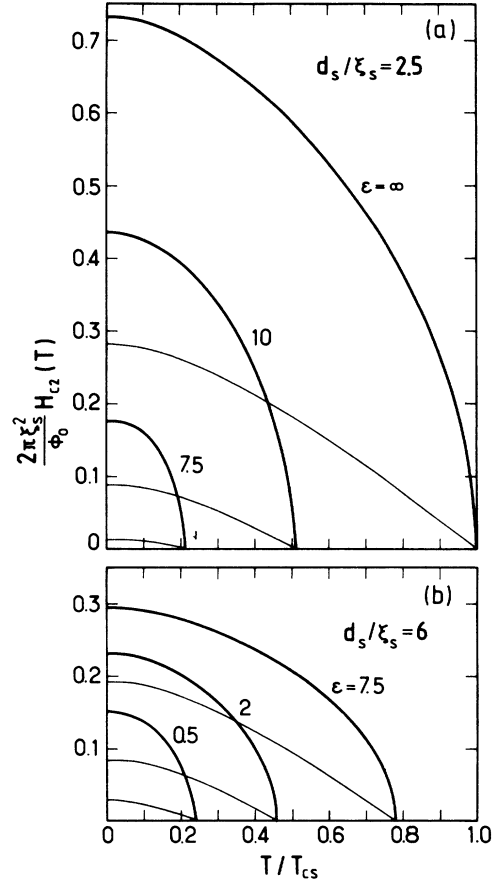


FIG. 4. Reduced upper critical fields $2\pi\xi_S^2 H_{c2}/\Phi_0$, both parallel (heavy curves) and perpendicular (light curves), as functions of the reduced temperature T/T_{cS} for (a) $d_S/\xi_S = 2.5$ and (b) $d_S/\xi_S = 6$, and for different values of ϵ .

$\rho(t) - \rho(t_c)$ are linear, is clearly seen. Note that for d_S close to d_{Sc} , such that $t_c < 0.5$, both $H_{c2\parallel}(0)$ and the slope $(-dH_{c2\parallel}^2/dT)_{T_c}$ increase rapidly with d_S (See Fig. 5). This effect, which is observed in Mo/Ni superlattices,⁴ is connected with the corresponding rapid variation of T_c with d_S . For thicker films, $t_c > 0.7$, the thickness dependence approaches the law $H_{c2\parallel} \propto 1/d_S$, as for the single thin film in vacuum. In our approach, the latter case corresponds to $\eta = 0$ ($\epsilon = \infty$), and hence $g(\phi_0) = 1$, and $\rho(t_c) = 0$, $t_c = 1$. In the vicinity of T_c , Eq. (20) reduces now to the well-known Ginzburg-Landau result,¹⁴ $H_{c2\parallel}(T) = \sqrt{12}\Phi_0/2\pi d_S \xi(T)$, and at low temperature to the result of de Gennes and Tinkham,¹⁵

$$H_{c2\parallel}(0) = 0.832\sqrt{12}\Phi_0/2\pi d_S \xi(0),$$

obtained by the correlation function method and valid for $l \lesssim d_S$, where l is the electronic mean free path. These results are valid up to the thickness $d_S = 1.84\xi(T)$ at which the vortices appear in the film.⁵ However, the nucleation of vortices in S/M multilayers starts at d_S considerably larger, since the superconductivity is suppressed near the S/M interfaces.

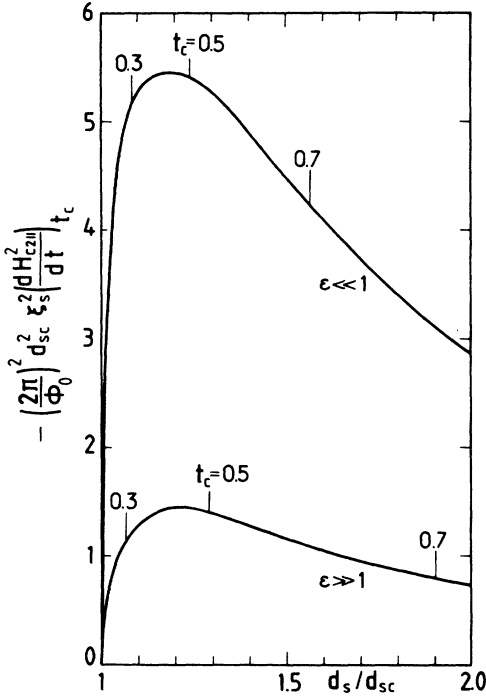


FIG. 5. Thickness dependence of the slope $-(dH_{c2||}^2/dt)_{t_c}$, calculated as $-H_{c2||}^2(t_c/2)/(t_c/2)$ in two limiting cases: $\epsilon \ll 1$ (upper curve) and $\epsilon \gg 1$ (lower curve).

IV. PERPENDICULAR CRITICAL FIELD

When the applied field is perpendicular to the layers, the magnetic flux penetrates through the superlattice in form of Abrikosov vortices, whose cores are strongly modulated in the field direction. The perpendicular critical field $H_{c2\perp}$ is given by the generalized de Gennes-Werthamer equation, as in the case of S/N superlattice,⁸

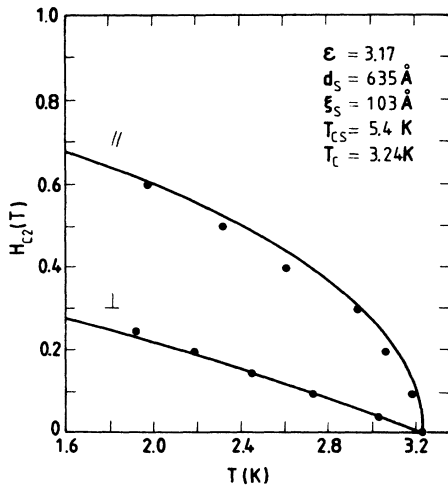


FIG. 6. Upper critical fields $H_{c2||}$ and $H_{c2\perp}$ vs T . The points are experimental data for V/Fe multilayer with $d_V=297$ AP and $d_{Fe}=9.8$ AP (Ref. 2). The theoretical curves are calculated using the parameters listed in the figure.

$$q_S \tan \left[\frac{q_S d_S}{2} \right] = \eta q_M \tanh \left[\frac{q_M d_M}{2} \right], \quad (22)$$

with

$$q_S^2 = k_S^2 - 2\pi H_{c2\perp} / \Phi_0 \quad (23a)$$

and

$$q_M^2 = k_M^2 + 2\pi H_{c2\perp} / \Phi_0. \quad (23b)$$

Still assuming, as before, that $|k_M d_M/2| \gg 1$ and $|k_M|^2 \gg 2\pi H_{c2\perp} / \Phi_0$, from Eq. (22) we obtain

$$\frac{q_S d_S}{2} \tan \left[\frac{q_S d_S}{2} \right] = (1+i) \frac{d_S / \xi_S}{\epsilon}. \quad (22')$$

From this equation, which is identical to Eq. (17), we find $q_S d_S/2 = \phi_0$ and using Eq. (23a) we obtain

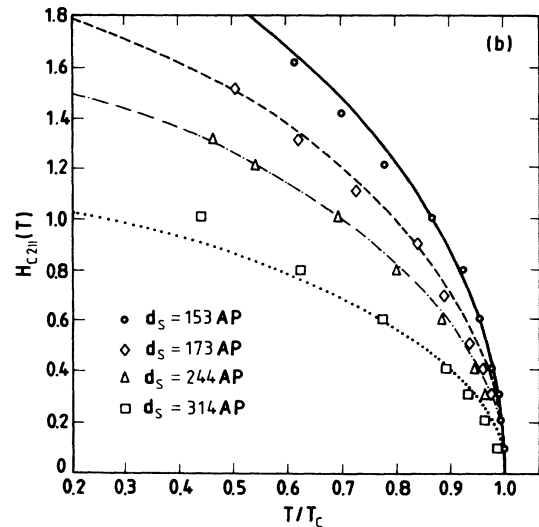
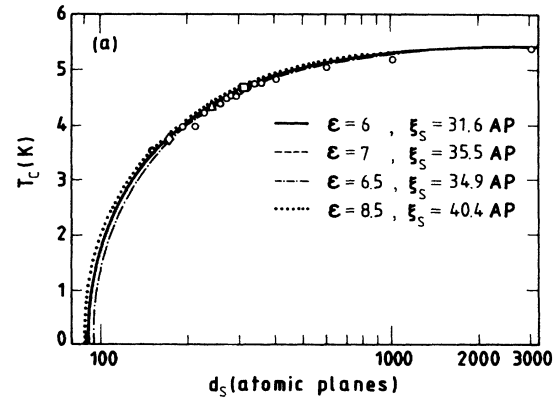


FIG. 7. Comparison with the experimental data for Fe/V/Fe sandwiches (Ref. 3): (a) T_c vs d_S and (b) $H_{c2||}$ vs T/T_c . For the chosen four values of the vanadium film thickness d_S , the theoretical curves are calculated taking $T_{cS}=5.4$ K and the atomic plane distance 2.14 Å, for ϵ and ξ_S listed in the figure.

$$\rho(t) = \rho(t_c) + \frac{\pi H_{c2\perp}}{\Phi_0} \xi_S^2. \quad (24)$$

Here the proximity effect enters only through $\rho(t_c)$, given by Eq. (18). The linear dependence of $H_{c2\perp}$ on $(1 - T/T_c)$ in the vicinity of T_c is clearly seen from Fig. 4. In the limit $d_S \rightarrow \infty$ or $\epsilon \rightarrow \infty$, and hence $\rho(t_c) \rightarrow 0$ and $t_c \rightarrow 1$, Eqs. (24) and (7) give, as expected, the bulk upper critical field H_{c2} . From Eqs. (20) and (24) one can see that the ratio $H_{c2\parallel}^2/H_{c2\perp}$ is temperature independent. For two limiting cases when $g(\phi_0)$ is real we have the simple relation

$$\frac{H_{c2\parallel}^2(T)}{H_{c2\perp}(T)} = \frac{\Phi_0}{d_S^2} \begin{cases} 6/\pi, & \frac{\epsilon \xi_S}{d_S} \rightarrow \infty \\ \frac{6/\pi}{1 - 6/\pi^2}, & \frac{\epsilon \xi_S}{d_S} \rightarrow 0. \end{cases} \quad (25)$$

This is a feature common to multilayered superconductors with decoupled thin S layers, so that no vortices nucleate in parallel field.

V. COMPARISON WITH EXPERIMENT

The square-root dependence of $H_{c2\parallel}$ on $(T_c - T)$ and the temperature-independent ratio $H_{c2\parallel}^2/H_{c2\perp}$ have been observed² in V/Fe superlattices for $d_S = 297$ AP (atomic planes) and $d_M = 9.8$ AP with $T_c = 3.24$ K. Taking the bulk value $T_{cS} = 5.4$ K and atomic plane distance of $3.02 \text{ \AA}/\sqrt{2} = 2.14 \text{ \AA}$ for vanadium bcc(110) structure,^{2,3} we find that the theoretical curves $H_{c2\parallel}(T)$ and $H_{c2\perp}(T)$ for $\epsilon = 3.17$ and $\xi_S = 103 \text{ \AA}$ are in good agreement with the experimental ones (see Fig. 6).

In Fe/V/Fe sandwiches,³ the 2D behavior in the temperature dependence of $H_{c2\parallel}(T)$ has been observed for d_S varying from 153 AP to 314 AP. A good agreement of both $T_c(d_S)$ and $H_{c2\parallel}(T, d_S)$ theoretical curves with the experimental data is obtained for $T_{cS} = 5.4$ K and for ϵ varying with d_S from 6 to 8.5 and ξ_S from 68 \AA to 86 \AA (see Fig. 7). The increase of ξ_S with d_S is consistent with the residual resistivity data,³ indicating the increase of the mean free path l with d_S , the values of ξ_S being consistent with H_{c2} data for bulk V.²

The 2D behavior of $H_{c2\parallel}(T)$, and an extremely rapid variation of T_c with d_S , were also observed⁴ in two short-period Mo/Ni superlattices with $d_S = d_M < 10 \text{ \AA}$. However, in this case the quantitative agreement between theory and experiment would require unrealistic large values of ξ_S .

In conclusion, thin S films in proximity of M metals do behave quite differently from isolated thin S films as seen from d_S dependences of T_c and $H_{c2}(T)$, and from the fact that the vortices start to nucleate^{2,3} at thicknesses considerably larger than $1.84\xi(T)$. Also, the decoupled behavior of S/M superlattices is in sharp contrast with that of finely layered S/N superlattices where near T_c the superconductor inherently averages over many layers.

ACKNOWLEDGMENTS

This work is supported in part by Grant No. JFP-520 under the National Science Foundation's U.S.-Yugoslavia Cooperative Research Program, and in part by Ames Laboratory operated for the Department of Energy by Iowa State University under Contract No. W-7405-Eng-82.

- ¹S. T. Ruggiero and M. R. Beasley, in *Synthetic Modulated Structures*, edited by L. Chang and B. C. Giessen (Academic, New York, 1984).
²H. K. Wong, B. Y. Jin, H. Q. Yang, J. B. Ketterson, and J. E. Hilliard, *J. Low Temp. Phys.* **63**, 307 (1986).
³H. K. Wong and J. B. Ketterson, *J. Low Temp. Phys.* **63**, 139 (1986).
⁴C. Uher, J. L. Cohn, and I. K. Schuller, *Phys. Rev. B* **34**, 4906 (1986).
⁵V. G. Kogan, *Phys. Rev. B* **34**, 3499 (1986); H. J. Fink, *Phys. Rev.* **177**, 732 (1969).
⁶S. Takahashi and M. Tachiki, *Phys. Rev. B* **33**, 4620 (1986).
⁷G. Eilenberger, *Z. Phys.* **214**, 198 (1968); K. Usadel, *Phys. Rev. Lett.* **25**, 507 (1970).
⁸K. R. Biagi, V. G. Kogan, and J. R. Clem, *Phys. Rev. B* **32**,

7165 (1985).

- ⁹A. I. Buzdin, L. N. Bulaevskii, and S. V. Panjukov, *Zh. Eksp. Teor. Fiz.* **87**, 299 (1984) [*Sov. Phys.—JETP* **60**, 174 (1984)].
¹⁰L. Dobrosavljević-Grujić and Z. Radović, *J. Appl. Phys. Jpn.* **26**, Suppl. 26-3, 1463 (1987).
¹¹K. Maki, in *Superconductivity*, edited by R. D. Parks (Dekker, New York, 1969), Vol. 2, p. 1035.
¹²G. Deutscher and P. G. de Gennes, in *Superconductivity*, edited by R. D. Parks (Dekker, New York, 1969), Vol. 2, p. 1005.
¹³L. J. Slater, *Confluent Hypergeometric Functions* (University of Cambridge Press, Cambridge, 1960), p. 70.
¹⁴V. L. Ginzburg and L. D. Landau, *Zh. Eksp. Teor. Fiz.* **20**, 1064 (1950).
¹⁵P. G. de Gennes and M. Tinkham, *Physics* **1**, 107 (1964).